Journal of the Society for Cardiovascular Angiography & Interventions 4 (2025) 102503

JSCAI

The official journal of the Society for Cardiovascular Angiography & Interventions

Original Research

Deformation of Surgically Implanted Aortic Valves: CT Findings Prior to Valve-in-Valve Implantation and Association With Mechanism of Failure

Abdellaziz Dahou, MD, PhD [a,b,c,*], Vinayak Bapat, MD [d], Torsten P. Vahl, MD [e], Lauren Ranard, MD [e], Martin B. Leon, MD [e], Rebecca T. Hahn, MD [e], Susheel K. Kodali, MD [e], Isaac George, MD [e], Vivian G. Ng, MD [e], Tamim M. Nazif, MD [e], Nadira Hamid, MD [d], Jason Hochler, BS [b], Eric Wolff, BS [b], Jordan Busch, BS [b], Ziad A. Ali, MD, DPhil [b], George Petrossian, MD [f], Newell Robinson, MD [f], Matthew Henry, MD [f], Jaffar M. Khan, MD, PhD [b,f], Omar Khalique, MD [a,b]

[a] *Division of Cardiovascular Imaging, St. Francis Hospital and Heart Center, Catholic Health, Roslyn, New York;* [b] *The DeMatteis Center for Cardiac Research and Education, Greenvale, New York;* [c] *Division of Cardiology, Massachusetts General Hospital/Harvard Medical School, Boston, Massachusetts;* [d] *Minneapolis Heart Institute, Minneapolis, Minnesota;* [e] *Structural Heart and Valve Center, Columbia University Medical Center, New York, New York;* [f] *Heart Valve Center, St. Francis Hospital and Heart Center, Roslyn, New York*

ABSTRACT

Background: Degeneration of surgically implanted bioprosthetic valves (BPVs) has been linked to risk factors including BPV construct and patient comorbidities. However, the role of the intrinsic structural configuration and potential structural changes of the surgical BPV itself on valve failure is unclear.

Methods: Patients who underwent cardiac computed tomography prior to aortic valve-in-valve due to surgical BPV failure were enrolled. Assessment included BPV ring dimensions, strut angles, strut-to-strut distance, and projected geometric orifice area (PGOA), defined as the area of the circle connecting the distal aspects of the struts. These measurements were compared with those of nonimplanted surgical BPVs matched for valve type and size. Echocardiograms were obtained before the valve-in-valve procedure, and valve structure and function were assessed. Mechanism of BPV failure was classified as aortic stenosis, aortic regurgitation, or mixed.

Results: A total of 222 patients were included. Aortic stenosis occurred in 111 (50%), aortic regurgitation in 55 (24.8%), and mixed in 56 (25.2%). Moderate/severe ring deformation (eccentricity index >10%) was present in 17% of cases. Strut angles, strut-to-strut distance, and PGOA were all significantly smaller in implanted than in reference valves (all $P < .0001$). The greatest average strut angle decrease was seen in Mitroflow valves (10°, $P < .0001$). The Mitroflow valve had the highest reduction in PGOA (27.7%), followed by Hancock (15.1%) and Perimount (11.6%; $P < .0001$). Smaller ring dimensions, smaller PGOA, and smaller strut-to-strut distance were associated with failure by stenosis (all $P < 0.05$) in univariable but not multivariable analysis.

Conclusions: Potential intrinsic changes (frame deformation) affect stented surgical BPVs implanted in aortic position. Whether these changes are associated with early valve degeneration and failure remains unknown.

Introduction

Nearly 280,000 prosthetic heart valves are implanted each year worldwide of which approximately 80% are bioprosthetic valves (BPVs).[1] Surgical aortic valve replacement (SAVR) is the historic gold standard of aortic valve replacement, and the number of SAVRs performed in the United States and worldwide remains high despite the emergence of transcatheter aortic valve replacement as an alternative option to surgery in high-, intermediate-, and low-risk patients.[2] BPVs have the advantage of no requirement for chronic anticoagulation. However, structural valve deterioration is an unavoidable complication during the lifetime of a BPV, with the need for reintervention with either redo SAVR or transcatheter valve-in-valve (ViV) for failing valves.[3] Structural deterioration of BPVs surgically implanted in aortic position

Abbreviations: AR, aortic regurgitation; AS, aortic stenosis; BPV, bioprosthetic valve; CT, cardiac computed tomography; EI, eccentricity index; PGOA, projected geometric orifice area (of the stent); SAVR, surgical aortic valve replacement; ViV, valve-in-valve.

Keywords: aortic valve; bioprosthetic valve deformation; cardiac computed tomography scan; Doppler echocardiography; structural valve degeneration; surgical aortic valve replacement.

* Corresponding author: dahouaziz1@gmail.com (A. Dahou).

https://doi.org/10.1016/j.jscai.2024.102503
Received 19 August 2024; Received in revised form 13 October 2024; Accepted 3 December 2024; Available online 13 March 2025

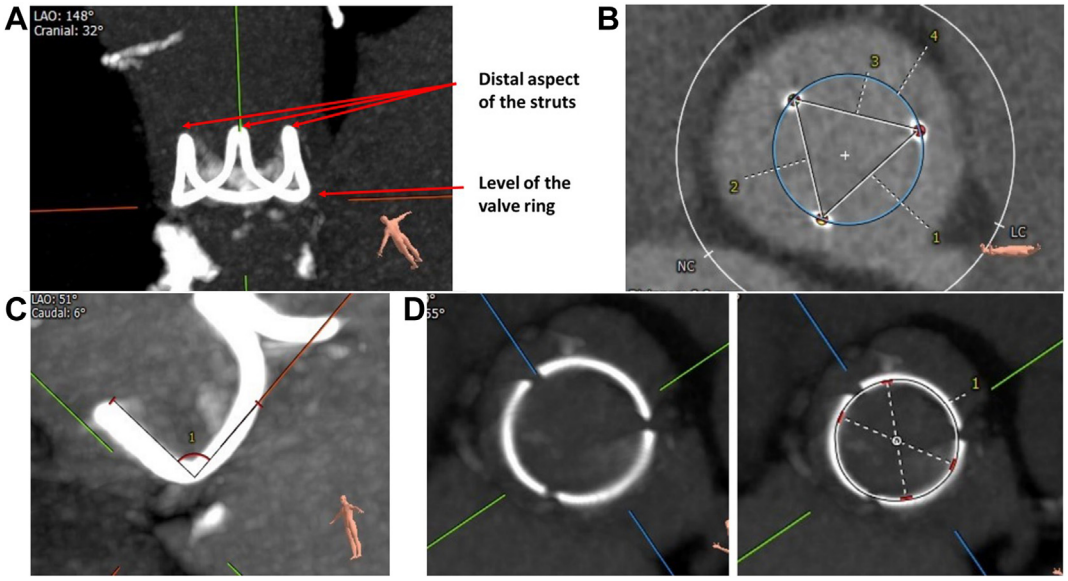

Figure 1.
CT scan measurements of a normally looking stented bioprosthetic valve. (A) Appearance of a stented bioprosthetic valve on CT scan. The struts of the stent and the valve ring are highlighted. (B) PGOA and strut-to-strut distance measurements: normally looking struts with similar strut-to-strut distances (1, 2, 3) (~19 mm). PGOA (blue circle) = 377 mm^2 (diameter: 21.9 mm). (C) Example of strut angle measurement. 1: Anteromedial angle = 91°. (D) Measurements of a normally looking ring. Inner min and max diameters: 20.7 × 20 mm, inner ring area: 325 mm^2, inner ring perimeter: 64 mm. CT, cardiac computed tomography; PGOA, projected geometric orifice area.

has been linked to a number of risk factors that can be related to the associated comorbidities, including an unfavorable metabolic profile and the presence of calcifications of the prosthetic valve leaflets during the first few years after SAVR.[4] However, the role of the intrinsic structural configuration and the potential changes of the BPV itself on SAVR failure is unknown.

Recent studies have shown that deformation of transcatheter heart valves is common and may result in a higher incidence of hypoattenuating leaflet thickening and poor outcome despite the absence of association with valve hemodynamics.[5] Deformation of the surgical BPV has been documented to frequently occur in normally functioning valves.[6] Little is known regarding deformation of surgical BPVs and its impact on the hemodynamic function and the durability of the valve. The present study aimed to investigate cardiac computed tomography (CT)-imaged BPV deformation following SAVR and its association with the mechanism of valve failure.

Table 1. Patient characteristics.

Variables	N = 222
Age, y	78 ± 11
Male sex	146 (66%)
Doppler echocardiography data	
LVEDd, cm	5.2 ± 0.9
LVEF, %	54 ± 13
LVSV, mL	80 ± 25
AVMG, mm Hg	32 ± 15
AVA, cm^2	1.05 ± 0.49
Valve type	
CE Perimount	95 (42.8%)
Magna	37 (16.7%)
Trifecta	33 (14.9%)
Mosaic	25 (11.2%)
Biocor	17 (7.6%)
Mitroflow	9 (4%)
Hancock	4 (1.8%)
CE Standard	2 (1%)
Valve size	
19 mm	30 (13.5%)
21 mm	40 (18%)
23 mm	78 (35%)
25 mm	52 (23.5%)
27 mm	20 (9%)
29 mm	2 (1%)

Data are presented as mean ± SD or n (%).
AR, aortic regurgitation; AS, aortic stenosis; AVA, aortic valve area; AVMG, aortic valve mean gradient; LVEDd, left ventricular end-diastolic diameter; LVEF, left ventricular ejection fraction; LVSV, left ventricular stroke volume.

Methods

Patient population

Patients who underwent CT between January 2014 and May 2022 prior to an aortic ViV procedure due to failure of surgical BPV from 2 high-volume centers (St. Francis Hospital and Columbia University Medical Center, New York) were enrolled. Demographics and echocardiographic and CT data were obtained for each patient. Only patients who had structural valve deterioration were included in this study. Patients with stentless valves and those with suboptimal echocardiograms or CT scans were excluded (Central Illustration). The research reported adhered to the relevant ethical guidelines, and patient consent was obtained, if needed.

CT assessment

In vitro CT imaging of bioprosthetic surgical valves of different types and sizes (n = 65), similar to those implanted in patients, was performed by placing the valves directly onto the table of a Siemens Somatom Flash Dual Source Scanner. Contrast CT images of in vivo BPVs were acquired using a Toshiba Aquilion One 320 detector row CT scanner at each institution. CT analysis was carried out using 3mensio software version 9.2-10.3, and the analyst was blinded to the clinical and echocardiographic data of the patients. Systolic phase (45%) was used for the reported measurements in all patients. Alignment of the bioprosthesis for measurements was performed in the

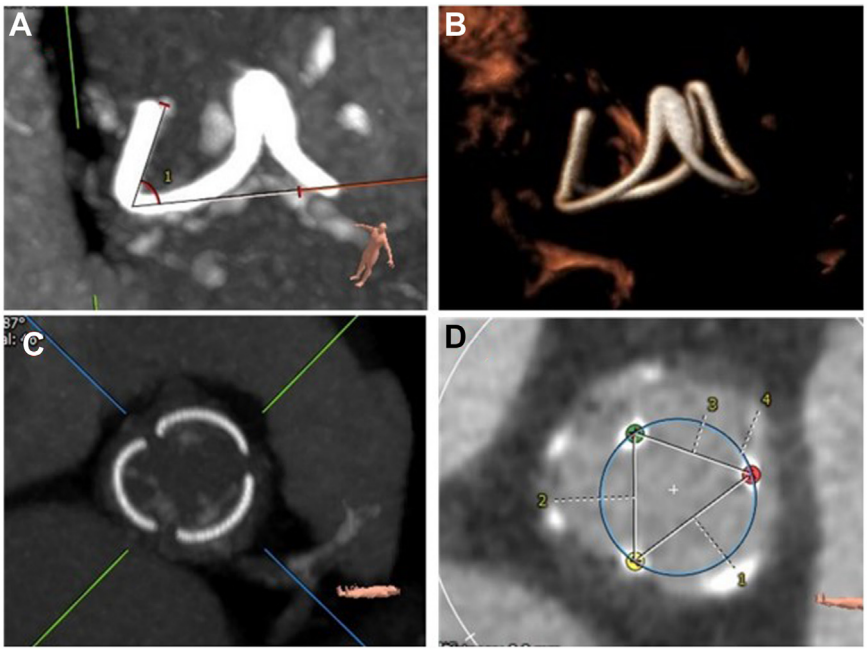

Figure 2.
Severely distorted strut. (A) Markedly distorted strut with reduced anteromedial angle (66°). (B) Same valve (Perimount 21 mm implanted in a small aortic annulus [20.7 × 23.3 mm]) with 3D appearance on CT scan. (C) Slightly deformed ring of the same valve. (D) Strut-to-strut distance is the smallest between the anteromedial (AM) and the anterolateral (AL) struts (distance 3 = 12 mm) due to strut distortion/angulation. Blue circle represents projected geometric orifice area of the stent; small green circle: AM aspect; small red circle: AL aspect; small yellow circle: posterior aspect. Images are representative of the same valve (same patient, same CT scan). CT, cardiac computed tomography.

same manner for in vivo and in vitro valves. A full maximum intensity projection of the prosthesis was used to align the basal sewing ring in one plane to ensure no parallax was present. CT assessment of the surgical BPVs included ring dimensions, ring area and perimeter, strut angles (anteromedial: AM, anterolateral: AL, and posteroseptal: PS), strut-to-strut distance, and projected geometric orifice area (PGOA) of the stent, which was defined as the area of the circle connecting the 3 distal aspects of the struts of the valve stent (Figure 1). In addition, the canting angle of the valve, which reflects the misalignment of the valve with the aortic root, was assessed. CT measurements were taken using a maximum intensity projection with a window width of 3000 and center of 1500. The eccentricity index (EI) of the valve ring was calculated as a measure of valve deformation as (1 − [minimal inner ring diameter / maximal inner ring diameter]) × 100. An EI <5% was

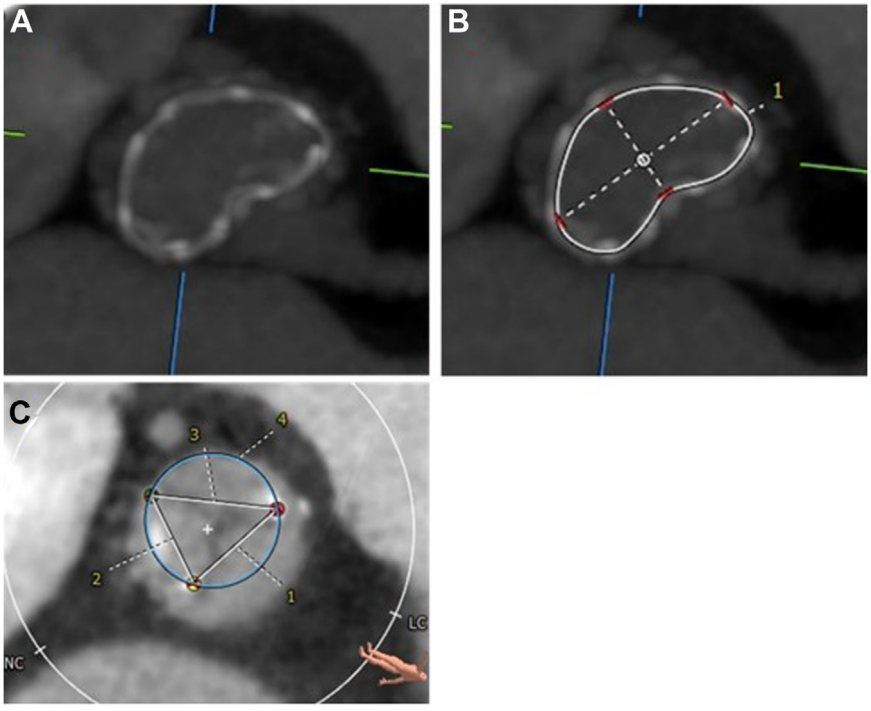

Figure 3.
Severely deformed ring. (A, B) Severely deformed ring with maximum diameter =19 mm and minimum diameter = 10 mm (ratio = 1.9 and eccentricity index >10%) in a Trifecta 19 mm valve. (C) Distorted struts resulting in significantly shorter strut-to-strut distance 2 (11.8 mm) as compared with distance 1 (13.6 mm) and distance 3 (15.4 mm). Projected geometric orifice area of the stent (blue circle): 200 mm^2. Images are representative of the same valve (same patient, same cardiac computed tomography scan).

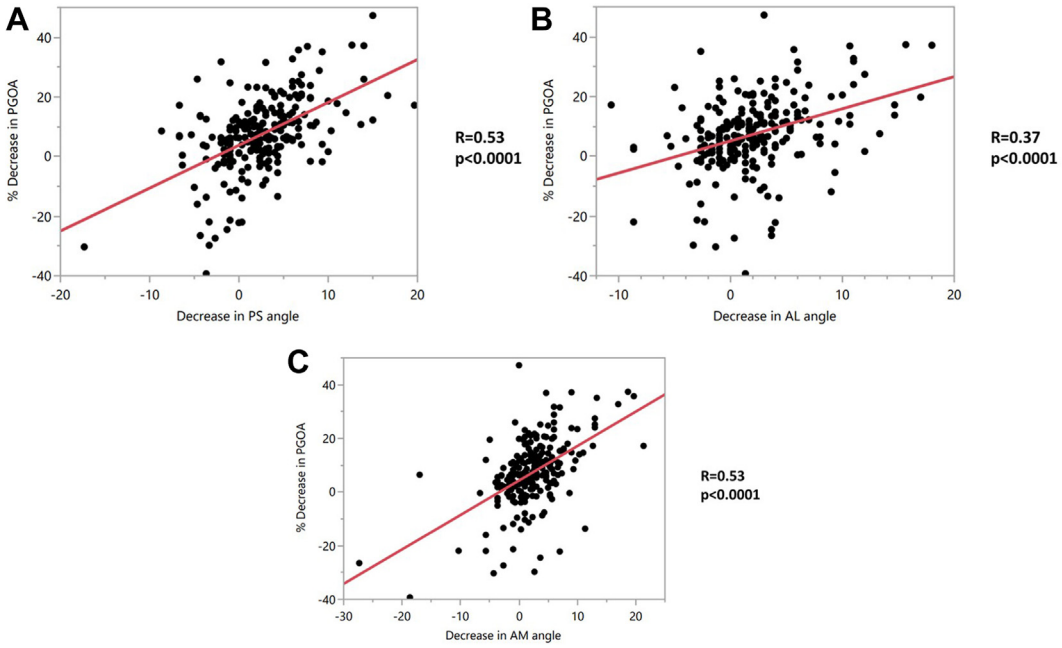

Figure 4.
Correlation between the changes in strut angles and the changes in PGOA. (A-C) Correlation between the changes in PS (A), AL (B), and AM (C) angles and the changes in PGOA. AL, anterolateral; AM, anteromedial; PGOA, projected geometric orifice area of the stent; PS, posteroseptal.

considered as none/trivial deformation (ie, circular ring), 5% to 10% as mild deformation, and >10% as moderate/severe deformation (ie, noncircular ring), as previously reported in the literature.[6–8] A decrease in strut angle ≥10° was considered meaningful. The CT measurements of the implanted valves were compared to in vitro CT measurements of out of the box nonimplanted surgical BPVs (ie, reference), with paired comparisons matched for the type and size for each valve. Additional CT measurements included the dimensions of the native neoaortic annulus, sinus of Valsalva, and sinotubular junction.

All CT measurements were performed by a single analyst, the first author (A.D.), who received dedicated training for this purpose and was supervised by the leading author (O.K.). Measurements were checked for accuracy by O.K., an expert in the field. Furthermore, intra- and interobserver variability assessments were performed and showed low (<5%) variability for both intra- and interobserver measurements. In particular, intra- and interobserver variability was 1.7% and 3.3%, respectively, for the PGOA of the stent, 1.8% and 2.9% for the stent angles, and 1% and 2% for the ring dimensions.

Doppler echocardiography

Echocardiograms were obtained for each patient prior to the ViV procedure, and valve structure and function were assessed using transesophageal echocardiography, transthoracic echocardiography, or both. Chamber quantifications and valvular function were carried out according to current guidelines.[9,10] The mechanism of failure of the surgical BPVs was classified as stenosis (aortic stenosis predominant: AS), regurgitation (aortic regurgitation predominant: AR), or mixed, with both significant stenosis and regurgitation (at least moderate of each).

Table 2. Paired comparison between out of the box, nonimplanted valves (reference) and surgically implanted valve measurements, matched for type and size

Variables	Out of the box valves (reference) (n = 65)	Implanted valves (n = 222)	*P*
Ring			
Ring perimeter-inner, mm	65.1 ± 7.4	65.3 ± 7.8	.40
Ring area-inner, mm^2	340 ± 77	342 ± 82	.59
Min ring diameter-inner, mm	20.0 ± 2.4	19.9 ± 2.5	.54
Max ring diameter-inner, mm	21.4 ± 2.4	21.5 ± 3.1	.12
Max/min ratio-inner	1.07 ± 0.02	1.08 ± 0.01	.046
Eccentricity index	6.57 ± 1.93	7.32 ± 5.14	.047
Struts + GOA			
Projected GOA, mm^2	342 ± 71	321 ± 78	< .0001
Projected GOA-min diam, mm	20.7 ± 2.2	20.0 ± 2.4	< .0001
Projected GOA-max diam, mm	20.9 ± 2.2	20.1 ± 2.4	< .0001
Strut angle-PS, °	89 ± 2	86 ± 5	< .0001
Strut angle-AL, °	89 ± 2	87 ± 5	< .0001
Strut angle-AM angle, °	89 ± 2	86 ± 6	< .0001
Strut-to-strut distance P-AL, mm	18.0 ± 1.9	17.3 ± 2.3	< .0001
Strut-to-strut distance P-AM, mm	18.1 ± 1.9	17.2 ± 2.2	< .0001
Strut-to-strut distance AL-AM, mm	18.2 ± 2.0	17.7 ± 2.3	< .0001

Data are presented as mean ± SD.
AL, anterolateral; AM, anteromedial; GOA, geometric orifice area of the stent; P, posterior; PS, posteroseptal.

Table 3. Changes in strut angles and projected GOA after valve implantation according to valve type.

Variables	Biocor (n = 17)	CE Stand. (n = 2)	Hancock (n = 4)	Magna (n = 37)	Mitroflow (n = 9)	Mosaic (n = 25)	Perimount (n = 95)	Trifecta (n = 33)	*P*
Strut angles									
Reference (average)	91 ± 1	86 ± 0.5	87 ± 0.5	88 ± 1	88 ± 0.3	87.0 ± 1.4	88.0 ± 1.3	90.5 ± 0.9	–
Implanted valves									
Strut angle-PS	89 ± 4	84 ± 9	86 ± 6	86 ± 4	76 ± 5[a]	88 ± 6	85 ± 4	89 ± 3	< .0001
Strut angle-AL	89 ± 5	86 ± 5	86 ± 3	86 ± 3	79 ± 48[a]	87 ± 6	85 ± 4	90 ± 3	< .0001
Strut angle-AM	87 ± 9	87 ± 2	84 ± 6	84 ± 3	79 ± 7[a]	89 ± 9	85 ± 3	91 ± 4	< .0001
Δ Strut angle-PS	1.8 ± 3.9	2.5 ± 9.7	1.2 ± 5.9	2.6 ± 3.9	12.2 ± 4.7[a]	−1.5 ± 5.9	3.4 ± 3.8	1.5 ± 2.9	< .0001
Δ Strut angle-AL	2.5 ± 5.2	0.5 ± 4.5	0.7 ± 2.4	2.0 ± 2.9	9.8 ± 4.3[a]	−0.4 ± 5.3	2.9 ± 4.2	0.01 ± 2.6	< .0001
Δ Strut angle-AM	4.5 ± 9.1	−1.0 ± 0.9	3.4 ± 6.7	4.2 ± 3.4	9.4 ± 7.6[a]	−1.8 ± 8.9	3.2 ± 3.5	−0.2 ± 3.9	< .0001
Projected GOA									
Reference	307 ± 53	305 ± 38	326 ± 81	331 ± 74	302 ± 39	324 ± 77	372 ± 68	318 ± 57	–
Implanted valves									
PGOA	298 ± 42	285 ± 3	279 ± 105	317 ± 88	217 ± 44	333 ± 84	329 ± 68	306 ± 56	–
Δ PGOA, % reduction	1.6 ± 14.7	5.8 ± 10.7	15.1 ± 20	4.9 ± 12	27.7 ± 13.5[a]	−4.6 ± 17.4	11.6 ± 8.0	3.8 ± 5.7	< .0001

Data are presented as mean ± SD.
AL, anterolateral; AM, anteromedial; GOA, geometric orifice area of the stent; PGOA, projected geometric orifice area of the stent; PS, posteroseptal.

Statistical analysis

Continuous variables of implanted valves were compared to those of out of the box nonimplanted valves (reference) matched for the type and size using paired *t* test for continuous variables and McNemar's test for categorical variables. Among patients with implanted valves, comparison between subgroups was carried out using *t* test or analysis of variance for the continuous variables and χ^2 or Fisher exact test for the categorical variables, as appropriate. Nominal logistic regression was used to study the effect of CT measurements on the mechanism of the valve failure. A 2-sided *P* value <0.05 was considered statistically significant. Analyses were performed using JMP 16 software (JMP Statistical Discovery LLC).

Results

Patient characteristics

A total of 222 patients with a failing surgical BPV who had both CT scans and Doppler echocardiography assessments were included in this analysis. Mean age was 78 ± 11 years, and 66% were male. Mean aortic valve area was 1.05 ± 0.49 and mean gradient 32 ± 15 mm Hg. The mechanism of failure was AS in 111 (50%), AR in 55(24.8%), and mixed with both significant AS and AR in 56 (25.2%, Table 1). Among valve types, CE Perimount (n = 95, 43%) was the most common, and valves size 23 mm were the most frequently used (n = 77, 35%) in this cohort, followed by 25 mm (n = 52, 23%) and 21 mm (n = 40, 18%). Median time between valve implantation and valve failure was 10.2 years (IQR, 7.1-14.0).

Table 4. Changes in strut angles and projected GOA after valve implantation according to valve size.

Variables	<23 mm (n = 70)	≥23 mm (n = 152)	*P*
Ring			
Eccentricity index, %	8.2 ± 0.6	6.9 ± 0	.07
Strut angles			
Strut angle-PS	86.6 ± 4.8	86.0 ± 4.8	.36
Strut angle-AL	86.5 ± 5.2	86.6 ± 4.4	.83
Strut angle-AM	86.9 ± 5.2	85.9 ± 5.4	.20
Δ Strut angle-PS	2.8 ± 4.6	2.4 ± 4.8	.54
Δ Strut angle-AL	2.9 ± 4.8	1.7 ± 4.2	.06
Δ Strut angle-AM	2.5 ± 5.1	2.5 ± 5.4	.94
Projected GOA			
PGOA, mm^2	246 ± 40	356 ± 66	< .0001
Δ PGOA, mm^2	17 ± 36	24 ± 55	.37
Δ PGOA, % reduction	6.0 ± 14.7	5.7 ± 15.7	.90

Data are presented as mean ± SD.
AL, anterolateral; AM, anteromedial; GOA, geometric orifice area of the stent; PGOA, projected geometric orifice area of the stent; PS, posteroseptal.

Prevalence and severity of deformation observed in implanted valves as assessed by CT

Figure 1 shows the main CT measurements described in the Methods section, and Figures 2 and 3 show examples of strut and ring deformation, respectively. Strut angles were measured in 220 of the 222 implanted surgical BPVs. Overall, absolute decrease in strut angle was 2.6 ± 4.7 vs 2.1 ± 4.4° vs 2.5 ± 5.3° for PS, AL, and AM struts respectively ($P \geq .22$). A decrease in strut angle by ≥10° was observed in 6.3% (14/220) for PS strut angle, 6.8% (15/220) for AL angle, and 6.3% (14/220) for AM angle. As a result, 14.5% of implanted valves exhibited a decrease by ≥10° in at least one of the strut angles (Central Illustration). In 5%, more than 1 strut angle had a decrease by ≥10°. Reduction in PGOA of implanted surgical BPVs by ≥10% as compared to the reference was present in 40%, while a decrease by >20% was seen in 14% of cases. There was a significant correlation between the changes in strut angles (absolute decrease in strut angles) and the relative changes in PGOA (percentage decrease in PGOA), with a correlation coefficient of 0.53 for both PS and AM angles and 0.37 for AL angle ($P <$ .0001 for all, Figure 4).

Regarding ring measurements, 25% had inner maximal-to-minimal ring diameter ratio ≥1.1, and 2.7% had a ratio ≥1.2. Two cases exhibited ratios of 1.9 and 2, respectively, suggesting extremely severe ring deformation (Figure 3). Overall, median EI was 6.3 (IQR, 4.7-9.0). EI was <5% in 29%, 5% to 10% in 54%, and >10% in 17% (Central Illustration). When compared according to valve size, EI tended to be higher in smaller valve sizes (<23 mm) than in larger valve sizes (≥23 mm): 8.2 ± 0.6% vs 6.9 ± 0.4%; $P = .07$. Furthermore, EI was significantly different among valve types ($P = .004$) being the highest in Mosaic (10.4 ± 1.0), CE Standard (10.4 ± 3.5), and Mitroflow (10.2 ± 1.6) and the lowest in Hancock (5.5 ± 2.5) and Magna (5.8 ± 2.0). In a subset of patients (n = 77) who had CT assessment in both systolic and diastolic phases, there was no significant difference in EI between the 2 phases (systole: 7.6 ± 2.6%, diastole: 7.2 ± 2.9%; $P = .29$).

Comparison between implanted and reference valves

When comparing the implanted valves to the nonimplanted (reference) valves after matching for type and size, strut angles, strut-to-strut

Table 5. Comparison of CT measurements according to the mechanism of prosthetic valve failure.

Variables	Entire cohort (N = 222)	AS (n = 111)	AR (n = 55)	Mixed (n = 56)	*P*
Ring					
Ring perimeter-inner	65 ± 8	63 ± 8	68 ± 7	66 ± 8	.0005
Ring area-inner	342 ± 82	322 ± 80	369 ± 76	352 ± 80	.0007
Min ring diameter-inner	19.9 ± 2.5	19.3 ± 2.6	20.7 ± 2.2	20.2 ± 2.5	.0002
Max ring diameter-inner	21.5 ± 2.6	20.8 ± 2.5	22.4 ± 2.3	21.9 ± 2.5	.0003
Max/min ratio-inner	1.08 ± 0.09	1.08 ± 0.08	1.08 ± 0.04	1.09 ± 0.11	.79
Eccentricity index	7.32 ± 5.12	7.26 ± 5.0	7.42 ± 3.35	7.37 ± 6.62	.97
Ring perimeter-mid	69 ± 8	67 ± 8	72 ± 7	70 ± 8	.0002
Ring area-mid	384 ± 89	362 ± 87	418 ± 88	394 ± 84	.0003
Ring center-min diameter	21.2 ± 2.6	20.6 ± 2.6	22.1 ± 2.3	21.4 ± 2.5	.0007
Ring center-max diameter	22.8 ± 2.6	22.1 ± 2.6	23.8 ± 2.5	23.1 ± 2.5	.0001
Struts					
Strut angle-PS	86 ± 5	86 ± 4	85 ± 6	86 ± 5	.33
Strut angle-AL	87 ± 5	86 ± 4	86 ± 5	87 ± 5	.62
Strut angle-AM	86 ± 6	87 ± 5	86 ± 5	85 ± 7	.52
Δ Strut angle-PS	2.6 ± 4.7	2.3 ± 3.9	3.2 ± 5.9	2.4 ± 4.9	.48
Δ Strut angle-AL	2.1 ± 4.4	2.4 ± 4.2	2.2 ± 4.8	1.5 ± 4.6	.49
Δ Strut angle-AM	2.5 ± 5.3	2.4 ± 5.3	2.7 ± 4.7	2.7 ± 5.9	.83
Strut-to-strut distance P-AL	17.3 ± 2.3	17.0 ± 2.0	17.7 ± 2.4	17.6 ± 2.5	.10
Strut-to-strut distance P-AM	17.2 ± 2.2	16.8 ± 2.1	17.7 ± 1.9	17.5 ± 2.7	.04
Strut-to-strut distance AL-AM	17.7 ± 2.3	17.2 ± 2.1	18.2 ± 2.3	18.0 ± 2.5	.01
PGOA	321 ± 78	306 ± 72	340 ± 77	330 ± 83	.01
Δ PGOA, % reduction	5.8 ± 15.3	5.6 ± 13.9	4.6 ± 17.5	7.2 ± 16.0	.68
Canting angle	6.9 ± 6.4	7.4 ± 6.1	5.8 ± 6.9	7.0 ± 6.6	.34
Native AV annulus					
AV annulus perimeter	80 ± 10	78 ± 9	84 ± 10	82 ± 10	.0001
AV annulus area	508 ± 122	476 ± 111	557 ± 124	523 ± 126	.0002

Data are presented as mean ± SD.
AL, anterolateral; AM, anteromedial; AR, aortic regurgitation; AS, aortic stenosis; AV, aortic valve; CT, cardiac computed tomography; P, posterior; PGOA, projected geometric orifice area of the stent; PS, posteroseptal.

distance, and PGOA were all significantly smaller in implanted valves than in the reference, nonimplanted valves (all $P < .0001$, Table 2), while ring dimensions including minimum and maximum diameters, perimeter, and area were not statistically different ($P \geq .12$). Furthermore, there was an interaction between the type of the valve and the changes in CT measurements between the implanted and reference valves, with the greatest decrease in strut angles seen in Mitroflow valves (decrease by 9°, 10°, and 12° for AM, AL, and PS strut angles, respectively; $P < .0001$), followed by Perimount (average decrease 3 ± 4°, Table 3). As a result, the Mitroflow valve had the highest relative decrease in PGOA (27.7 ± 13.5% reduction), followed by Hancock (15.1 ± 2% reduction) and Perimount (11.6 ± 8.0% reduction;

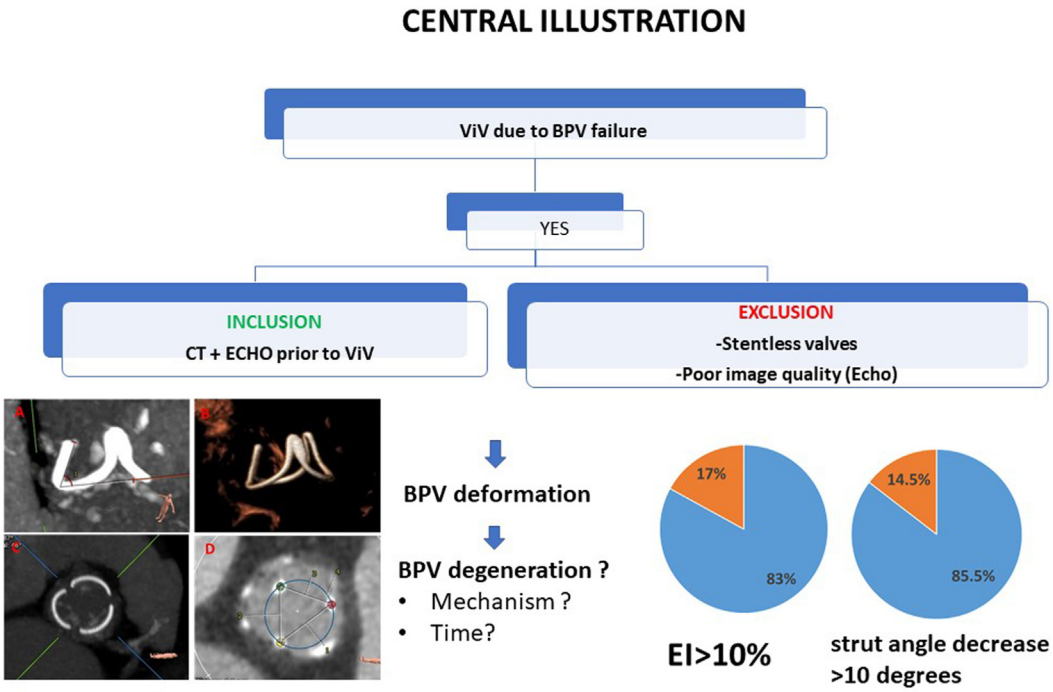

Central Illustration.
Deformation of surgically implanted aortic valves and potential association with valve degeneration and failure. BPV, bioprosthetic valve; CT, cardiac computed tomography; Echo, echocardiography; EI, eccentricity index; ViV, valve-in-valve.

$P < .0001$) while other valves had less decrease. When compared according to the size of the valve (≥23 mm vs <23 mm), there was no difference in the absolute and relative changes in strut angles and relative changes in PGOA between the 2 groups. As expected, smaller BPVs exhibited significantly smaller PGOA (Table 4).

Effect of CT-derived measurements on valve durability and mechanism of valve failure

When comparing time to valve failure according to the severity of ring eccentricity, there was no significant difference in time to failure between patients who had none/trivial, mild, and severe eccentricity (11.5 ± 4.8 vs 10.7 ± 5.2 vs 10.1 ± 3.8 years, respectively; $P = .46$). When compared according to the median value of EI (6.3%), valve durability represented by time to failure tended to be shorter in those with EI greater than the median versus those with EI less than the median (10.35 ± 4.51 vs 11.60 ± 5.0 years; $P = .12$).

Decrease in strut angle >10° of any of the strut angles was not associated with time to failure ($P \geq .24$). Smaller ring-derived measurements, smaller PGOA, and smaller strut-to-strut distance were associated with the mechanism of failure by stenosis in univariable analysis ($P < .05$ for all), whereas the absolute and relative changes in PGOA and strut angles were not (Table 5). After adjustment for valve type and size, and native aortic annulus area, none of the CT-derived measurements remained associated with the mechanism of failure.

Discussion

The main findings of the present study are as follows: (1) deformation of surgically implanted BPVs in aortic position is not rare; (2) surgically implanted BPVs in aortic position may exhibit structural changes including inward stent creep with subsequent decrease in strut angles and/or ring distortion; (3) a smaller strut-to-strut distance, smaller PGOA of the stent, and smaller ring dimensions were associated with valve degeneration by stenosis (AS) in univariable but not in multivariable analysis.

Only limited data exist regarding deformation of surgical BPVs implanted in aortic position. A recent study including 152 patients with surgical BPVs showed that surgical BPV deformation is quite common, with mild deformation or greater (EI > 5%) being present in 56% of cases and more severe deformation (EI > 10%) found in 17% of cases.[6] However, this study was limited to a descriptive analysis of the ring of the implanted valves, and there was no comparison with a reference. In our study, the assessment of the surgical BPVs was more comprehensive, and the implanted valves were compared to a reference. The results of the present study confirmed the finding of previous studies and suggest that the deformation can affect the struts of the stent, the valve ring, or both. This deformation/distortion may lead to abnormal leaflet function, flow disturbance, and suboptimal valvular hemodynamics, similar to what has been reported with underexpanded transcatheter valves.[11] In our study, a valve distortion resulting in a decrease in strut angle by 10° affecting at least one of the struts was quite common (~15%). Consequently, a reduction in PGOA of implanted surgical BPVs by ≥10% as compared with the reference was present in 40%, while a decrease >20% was seen in 14% of cases. Although decreased strut angle was not associated with mechanism of failure (AS vs AR vs mixed), smaller PGOA resulting from stent distortion was associated with degeneration of surgical BPVs due to stenosis as assessed by Doppler echocardiography. However, this association was no longer significant after adjustment for valve size and type. Whether the deformation of surgical BPVs would cause a deformation or underexpansion of subsequent transcatheter ViV remains to be demonstrated.

The causes of deformation of surgical BPVs remain unclear. However, unintentional deformation during surgery cannot be excluded, especially in patients with small aortic annuli for which implantation of an oversized valve in an attempt to get a larger aortic valve area can result in a more challenging procedure, which can, in turn, result in valve deformation. The results of the present study point toward this hypothesis, at least in cases with severe deformation, given the staggering degree of distortion of the struts or the ring noticed in some of our patients and the trend toward a higher eccentricity index in patients with smaller valve size. Such a deformation is unlikely to happen spontaneously. Furthermore, the use of minimally invasive surgical approaches to perform SAVR may lead to intentional deformation of the valve for a short period of time during valve implantation through a small opening between the ribs, assuming that this deformation (squeeze) is without consequence. Finally, it is unclear whether compression of the valve by surrounding structures such as the interventricular septum can lead to or aggravate valve deformation. We hypothesized that dynamic motion of the interventricular septum may result in or contribute to deformation of the valve, especially the anteromedial strut, which is anatomically more subject to compression by the interventricular septum. However, the results of the present study do not support this hypothesis, given that absolute decrease in strut angle as well as a decrease by ≥10° were similar between the 3 stent struts.

These findings may also suggest the need for considering additional procedural interventions such as aortic root enlargement when implanting surgical valves in small aortic annuli to achieve better valve hemodynamics without causing deformation of the implanted valve.

Strength and limitations

Our study has some limitations. First, the timing of valve deformation is unknown because no CT scans were available immediately after SAVR. However, this can be explained by the lack of indications to routinely perform a CT scan following SAVR. Second, our study included only patients with stented bioprosthetic surgical valves. Therefore, the findings of the present study are not generalizable to other valve types. Finally, we were not able to study the structural deformation in patients with normally functioning BPVs due to the lack of CT scanning after SAVR in most of these patients. Indeed, there is no indication to routinely perform a cardiac CT in these patients with otherwise normally functioning BPVs.

Conclusion

The results of the present study highlight the potential intrinsic structural changes that can affect stented surgical valves implanted in aortic position, including both stent and ring deformations. These changes are not rare and may result in a conflict between the struts of the stent and the valve leaflets. Whether these changes may be associated with an early structural valve deterioration and failure of these valves remains to be demonstrated. Further studies with serial CT scans and echocardiograms are needed to better characterize the natural history of these changes and their effect on the hemodynamic performance and durability of surgical BPVs.

Declaration of competing interest

Rebecca Hahn reports speaker fees from Abbott Structural, Baylis Medical, Edwards Lifesciences, Medtronic, Philips Healthcare, and Siemens Healthineers; she has institutional consulting contracts for which she receives no direct compensation with Abbott Structural, Edwards Lifesciences, Medtronic, and Novartis; and she is Chief Scientific Officer for the Echocardiography Core Laboratory at the Cardiovascular Research Foundation for multiple industry-sponsored valve trials, for which she receives no direct industry compensation. All other authors reported no financial interests.

Funding sources

This work was not supported by funding agencies in the public, commercial, or not-for-profit sectors.

Ethics statement and patient consent

The research reported adhered to the relevant ethical guidelines, and patient consent was obtained, if needed.

Peer Review Statement

Section Editor Ziad A. Ali had no involvement in the peer review of this article and has no access to information regarding its peer review. Full responsibility for the editorial process for this article was delegated to Associate Editor Andrew M. Goldsweig.

References

1. Pibarot P, Dumesnil JG. Prosthetic heart valves: selection of the optimal prosthesis and long-term management. *Circulation*. 2009;119(7):1034–1048.
2. Carroll JD, Mack MJ, Vemulapalli S, et al. STS-ACC TVT registry of transcatheter aortic valve replacement. *J Am Coll Cardiol*. 2020;76(21):2492–2516.
3. Kostyunin AE, Yuzhalin AE, Rezvova MA, Ovcharenko EA, Glushkova TV, Kutikhin AG. Degeneration of bioprosthetic heart valves: update 2020. *J Am Heart Assoc*. 2020;9(19):e018506.
4. Salaun E, Mahjoub H, Dahou A, et al. Hemodynamic deterioration of surgically implanted bioprosthetic aortic valves. *J Am Coll Cardiol*. 2018;72(3):241–251.
5. Fukui M, Bapat VN, Garcia S, et al. Deformation of transcatheter aortic valve prostheses: implications for hypoattenuating leaflet thickening and clinical outcomes. *Circulation*. 2022;146(6):480–493.
6. Faure ME, Suchá D, Schwartz FR, et al. Surgically implanted aortic valve bioprostheses deform after implantation: insights from computed tomography. *Eur Radiol*. 2020;30(5):2651–2657.
7. Willson AB, Webb JG, Gurvitch R, et al. Structural integrity of balloon-expandable stents after transcatheter aortic valve replacement: assessment by multidetector computed tomography. *J Am Coll Cardiol Intv*. 2012;5(5):525–532.
8. Caudron J, Fares J, Hauville C, et al. Evaluation of multislice computed tomography early after transcatheter aortic valve implantation with the Edwards SAPIEN bioprosthesis. *Am J Cardiol*. 2011;108(6):873–881.
9. Lang RM, Badano LP, Mor-Avi V, et al. Recommendations for cardiac chamber quantification by echocardiography in adults: an update from the American Society of Echocardiography and the European Association of Cardiovascular Imaging. *J Am Soc Echocardiogr*. 2015;28(1):1–39.e14.
10. Zoghbi WA, Adams D, Bonow RO, et al. Recommendations for noninvasive evaluation of native valvular regurgitation: a report from the American Society of Echocardiography developed in collaboration with the Society for Cardiovascular Magnetic Resonance. *J Am Soc Echocardiogr*. 2017;30(4):303–371.
11. Fukui M, Sorajja P, Cavalcante JL, et al. Deformation of transcatheter heart valve following valve-in-valve transcatheter aortic valve replacement: implications for hemodynamics. *J Am Coll Cardiol Intv*. 2023;16(5):515–526.